Materials Research Proceedings 29 (2023) 272-280 https://doi.org/10.21741/9781644902516-30

Activated carbon/graphene composite electrodes with green polymeric binder for carbon dioxide reduction: Preliminary study

MUHAMAD FARHAN HAQEEM Bin Othman[1,a], INTAN SYAFIQAH Ismail[1], MUHAMAD HAFIZHAN HAFIY Mohammad Azmi[2,] NOR ADILLA Rashidi[1,b*], SUZANA Yusup[3] and NORIDAH Osman[1,c]

[1]Chemical Engineering Department, Higher Institution of Center of Excellence: Centre for Biofuel and Biochemical Research, Institute of Self-Sustainable Building, Universiti Teknologi PETRONAS, 32610 Bandar Seri Iskandar, Perak, Malaysia

[2]Process & Process Safety, Exen International Sdn Bhd, Suite 10-23, Tower 1, Wangsa 118, Jalan Wangsa Delima, Wangsa Maju, 53300, Kuala Lumpur, Malaysia

[3]Generation Unit (Fuel & Combustion Section), Tenaga Nasional Berhad Research (TNBR), No1, Kawasan Institusi Penyelidikan, Jln Ayer Hitam, 43000 Kajang, Selangor, Malaysia

[a]farhanhaqeem123@gmail.com, [b]adilla.rashidi@utp.edu.my, [c]noridah.osman@utp.edu.my

Keywords: Carbon Dioxide Reduction, Activated Carbon-Graphene Oxide Composite, Green Polymeric Binder, Biopolymer, Electrocatalytic Reaction

Abstract: In the present study, a few types of green polymer binder such as Xanthan gum (XG), Carboxyl methylcellulose (CMC) and Sodium alginate (SA) have been prepared with activated carbon-graphene oxide composite electrode (AC/GO). Throughout the experiment, CMC as an individual polymeric binder produce the least amount of the weight loss (8.28%). To enhance the adhesion, the binder was mixed with synthetic binder (PEI), which results in mass loss of 1.86%. Furthermore, the electrochemical analysis depicts that AC/GO-SA produces the highest current rate (-7.8 mA/cm^{-2}) throughout the 30 min of reduction process, with 16.9% Faradaic efficiency. The experimental results show that a facile, low-cost, eco-friendly design of green polymer binder is promising for the carbon dioxide reduction, thus, promote a greener technology.

Introduction

Ever since the Industrial Revolution, anthropogenic carbon dioxide (CO_2) level in the atmosphere has continuously increasing from 280 ppm to over 400 ppm due to extensive fossil fuels burning [1]. Excessive consumption of fossil fuels has cautiously led to the depletion of these finite natural resources while rising the atmospheric CO_2 concentration. The increasing CO_2 concentration in the Earth's atmosphere has raised numerous of environmental concerns, such as global warming, rising sea level as well as species extinction, which all cause a significant disruption to the ecosystem [2]. The release of CO_2 into the environment is uncontrollable as a consequence of various current industrial processes. In contrast with the natural carbon cycle of having a closed loop process, the open loop of these anthropogenic activities which releases CO_2 into the environment is unsustainable. Minimizing the CO_2 emissions assist in solving the environmental issues such as switching to low carbon-fuel (hydrogen or syngas) or upgrading the energy efficiency and enhance the energy conservation [3].

Electrochemical reduction of CO_2 has attracted much attention in recent years as it represents a clean technique at the expense of facilitating sustainable supply for energy storage and conversion. This technique has the advantage where water can be used as the proton source and procedure can be carried out a room temperature. However, some issues need to be resolved before the electrochemical reduction of CO_2 becomes appealing for technological applications, related to the high efficiency and product selectivity [4]. The electrochemical approach mainly relates with

Content from this work may be used under the terms of the Creative Commons Attribution 3.0 license. Any further distribution of this work must maintain attribution to the author(s) and the title of the work, journal citation and DOI. Published under license by Materials Research Forum LLC.

measurement and control of a redox reaction in electrochemical cells. In electrochemical cells, electrodes are set into an electrolyte for chemical reaction to occur. The composite electrode is considered as one of the important configurations in electrochemical performance testing [1].

Typically, fabrication of composite electrode includes active material, polymer binder material and conductive material. As an improvement in the electrode fabrication, activated carbon electrode particularly the functionalization of active material and extensive performance of conductive material has gained many research interests, with minimal attention to improve the binder material. [5]. Binder plays an important role as the surfactant that binds the material altogether and control the functionality of the electrode. The binder forms a matrix for the active material and allows build-up contact with the current collector, which then provides mechanical durability. The binder has to be electrochemically stable, insoluble in the electrolyte solution, and must be evenly distributed in the slurry during the electrode fabrication. Common polymeric binder in electrochemical capacitor is based on fluorinated polymer like polyvinylidene fluoride (PVDF), polyvinyl alcohol (PVA) and Nafion. However, these polymer binders suffer atrocious drawbacks such as high toxicity and poor adhesion [6]. These fluorinated polymers often require wetting agents or organic solvents during the fabrication process and release fluorinated monomers which has severe environmental effects [7]. Thus, green polymeric binder is said to be a great alternative as it maintains the environmental concerns of reducing toxicity [8]. Derived from nature, Sodium Alginate (SA), Xanthan Gum (XG), and Carboxyl Methylcellulose (CMC) are the examples of green binders as substitute for electrode fabrication and the performance of each binder has been carried out and described in this study.

Experimental and methods

Chemicals and reagents

Green polymer such as carboxymethyl cellulose (CMC) (CAS No: 9000-11-7; Food grade), xanthan gum (XG) (CAS No: 11138-66-2; Food grade), and sodium alginate (SA) (CAS No: 9005-38-3; Food grade) were supplied by Take It Global Sdn Bhd, Penang, Malaysia. Activated carbon (AC) powder (from coconut shell) was acquired from Kekwa Indah Sdn Bhd, Negeri Sembilan, Malaysia. Graphene oxide (GO) solution (4 mg/mL, in H_2O), polyethylenimine (PEI) solution (50% in H_2O) and corn starch (CAS No: 99005-25-8) were supplied by Sigma Aldrich. Potassium hydroxide (KOH) and potassium bicarbonate ($KHCO_3$) (Chemically Pure Grade) were procured from the R&M Chemical. Copper (II) sulfate pentahydrate powder (CAS No: 7758-99-8), Sodium hydroxide pellets (CAS NO: 1310-73-2) and L (+) ascorbic acid powder (CAS No: 50-81-7) were purchased from Merck Millipore. All chemicals were used as supplied.

Catalyst synthesis and electrode fabrication

The synthesis of catalyst or material for the working electrode starts with the preparation of copper nanoparticle (CuNP) as a conductive material for the composite electrode. The chemical reduction process by using corn starch as capping agent was inspired from [9]. Next, the process continued with mixing all the material for composite electrode such as AC, GO (as active material), CuNP (as conductive material) and SA, XG, PEI and CMC (as polymer binder) in a one-pot synthesis with a composition ratio of 8:1:1 (active material: conductive material: binder).

Dipping layer-by layer technique was selected to fabricate the electrode; the detailed process was already been reported elsewhere [10], [11]. Four electrodes having the similar active and conductive material, but different polymer binder have been fabricated, and was labelled according to the type of binder, as: AC/GO-x where *x* represent the polymer binder (*x* = SA, XG, CMC and CMC/PEI). The CMC-PEI electrode used a mixed binder of green polymer with synthetic polymer at a ratio of 1:1 (CMC:PEI) as the ionic interaction of anionic polymer (CMC) and cationic polymer (PEI) during crosslinking process could improve the binding energy [12].

Physical and electrochemical measurement

Excess slurry of the coating material was dried at 50ºC overnight to obtain the catalyst in powder form for further characterization. The powder's structure was examined using Fourier Transmission Infrared Spectroscopy (FT-IR) with a wavelength ranged from 4000 to 400 cm^{-1}. The IR spectrum were detected by using a KBr disc to study effect of adding green polymer binder towards the AC-GO solution. Next, zeta potential for the green polymer was determined by using the Dynamic light scattering (DLS) with the Standard Operating Procedure of the DLS instrument.

The electrochemical measurement was carried out by using the H-cell, three electrodes setup with dual compartments, separated by Nafion 117 membrane and single-channel potentiostat (AUTOLABPGSTAT3002, Metrohm, Malaysia). The prepared electrodes act as a working electrode, with platinum coil as counter electrode and silver chloride served as reference electrode. Before and after each run, the working electrode mass was recorded to measure the percentage mass loss. The electrochemistry activity towards CO_2 reduction was determined using cyclic voltammetry (CV) and chronoamperometry (CA) analysis. The CV analysis was performed from 0 to -1.4V *vs.* Ag/AgCl applied potential to determine the onset potential for the CO_2RR. The CV was in both CO_2 and inert argon atmosphere with gas flow rate of 20 m^3/s. Later, the optimum potential will be selected and applied in CA for 30 min. Finally, the liquid product of the reaction was sent for FTIR and DLS analysis to study the surface properties of the materials.

Result and discussions

Surface properties

The FT-IR spectra of AC/GO-raw (without binder), AC/GO-CMC/PEI, AC/GO-SA, AC/GO-XG and AC/GO-CMC are illustrated in Figure 1. All of the composite shared a distinct peaks at 1075 and 3437 cm^{-1} which correspond to C-O and C-OH bonds in the carbon skeleton network [13]. For raw composite, the presence of oxygen-containing functional groups at peaks 1436 and 1719 cm^{-1} refers to the O-H bending of and C=O stretching of carboxyl group, respectively. According to [14], the absorption bands 1635 and 1436 cm^{-1} are assigned to the pyrrole ring vibrations which can only be clearly seen on the raw composite. The addition of polymer binder onto the composite clearly deforms the peaks of the pyrrole ring which attributed to C=C that indicates a good interaction between the AC/GO and the polymer binder. Moreover, peak at 2346 cm^{-1} is attributed to the O=C=O stretching which only clearly visible for AC/GO-CMC, AC/GO-CMC/PEI and AC/GO-XG. The broad peak at 3430 to 3420 cm^{-1} correspond to the hydroxyl (C-OH stretching) group. However, AC/GO-CMC/PEI shows a broader peak around 3434 cm^{-1} as compared to others due to the N-H stretching vibration from PEI solution [15]. All the functional groups detected promote intermolecular bonding such as covalent or hydrogen bond, which could possibly improve the active material adhesion.

Furthermore, the behavior of the green polymers is studied through the zeta-potential as it reflects the interpretation of the polymers and the charged of the polymers [16]. The value of zeta potential is important when dispersing the composite in aqueous solution to ensure the stability of the colloid in solution. The zeta potential for the green polymer composite (AC/GO-SA, AC/GO-XG and AC/GO-CMC) is shown in Figure 1 (b). Based on the analysis, AC/GO-CMC has the highest charge, followed by AC/GO-SA and AC/GO-XG with zeta-potential of -84.6, -75.2 and -27.5 mV, respectively.

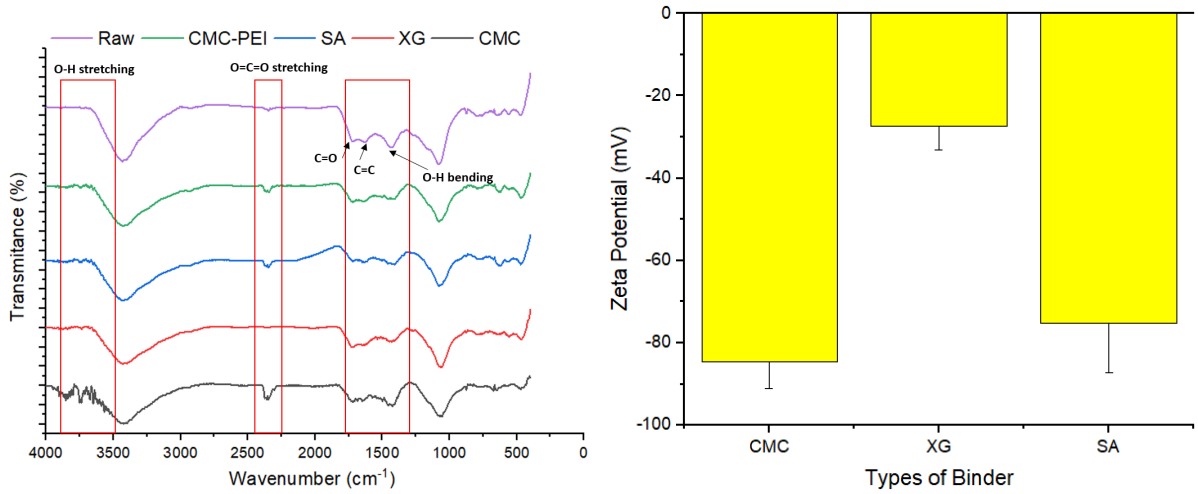

Figure 1: FTIR analysis was done to examine the chemical bonding of the composites (left), Zeta-potential of AC/GO-x (x= CMC; XG; and SA) solution (right).

According to [16], the charge of the green polymer can be increased by mixing different type of polymers could initiate mutual masking of surface charges among multiple polymers. Zeta-potential value higher than 60 mV is already considered as excellent stability except for AC/GO-XG which have zeta-potential value less than 30 mV which considered as incipient instability [17]. The higher the value of zeta potential, the more stable the dispersion is, as these particles repel each other and will prevent agglomeration during cross-linking process. Nevertheless, overall efficiency of the binder is still depending on the adhesiveness of the coating material between the current collector and composite materials.

To study the reusability of the fabricated electrodes, adhesiveness of the coating material is measured and recorded in Table 1. The mass of the fabricated electrode before and after the reduction reaction is recorded to calculate the percentage mass loss. Based on the results, AC/GO-XG has the highest mass loss with 19.89% followed by AC/GO-SA with 19.78% of mass loss. Further, AC/GO-CMC has the least mass loss with 8.28%; hence this supports the zeta potential findings shown in Figure 1 (b). To further improve the adhesiveness of the composite catalyst, mixed polymeric binder is being synthesized, as cationic and anionic interaction of CMC and PEI is expected to produce a positive impact to the adhesiveness. The concept of cross-linked binder is to enhance the characteristics of the binder, increase chemical stability and maximize acid-base interactions between material [18]. PEI solution is chosen as synthetic binder to be mixed with CMC (mixing ratio 1:1) as it has the ability to tune the carbon backbone in the AC-GO, and to promote the CO_2RR reaction [19]. Table 1 shows that AC/GO-CMC/PEI has the highest stability and recyclability electrode among others as it leached out the least (1.86%). This might due to the non-covalent dispersion interactions based on Van der Waals forces and hydrogen bonding which eliminates the hydrophobic interface of PEI with other materials [20]. Though, according to [21], determining optimum amount of polymeric binder is important as the surplus amount contributes to pore clogging and destruction of catalysts' active sites.

Table 1: Percentage mass loss of electrode in adhesiveness test.

Composites	Mass (g)		Percentage mass loss (%)
	Before	After	
AC/GO-SA	0.172	0.138	19.78
AC/GO-XG	0.191	0.153	19.89
AC/GO-CMC	0.145	0.133	8.28
AC/GO-CMC/PEI	0.161	0.158	1.86

Electrochemical measurement of CO_2 reduction

The CV analysis is performed at potential ranges of 0 to -1.4 V *vs.* Ag/AgCl at a scan rate of 50 mV/s, using 0.1M $KHCO_3$ as catholyte. The CV result is compared between CO_2 (red) and argon atmosphere (black) in order to observe the anodic shifting, and the findings are illustrated in Figure 2. Among all the electrodes, AC/GO-SA produces the highest current in the CO_2 atmosphere (-0.08 A) at potential of -1.4 V and followed by AC/GO-XG (0.045 A), AC/GO-CMC (0.04 A) and AC/GO-CMC/PEI (0.03 A). However, only the AC/GO-SA and AC/GO-CMC/PEI shows a clear anodic shifting whereas the other electrode produce the same current as in the inert atmosphere. Fundamentally, if the current produced is similar under the inert and CO_2 atmosphere, there is high possibility of dominant hydrogen (H_2) evolution, instead of the CO_2 evolution [22].

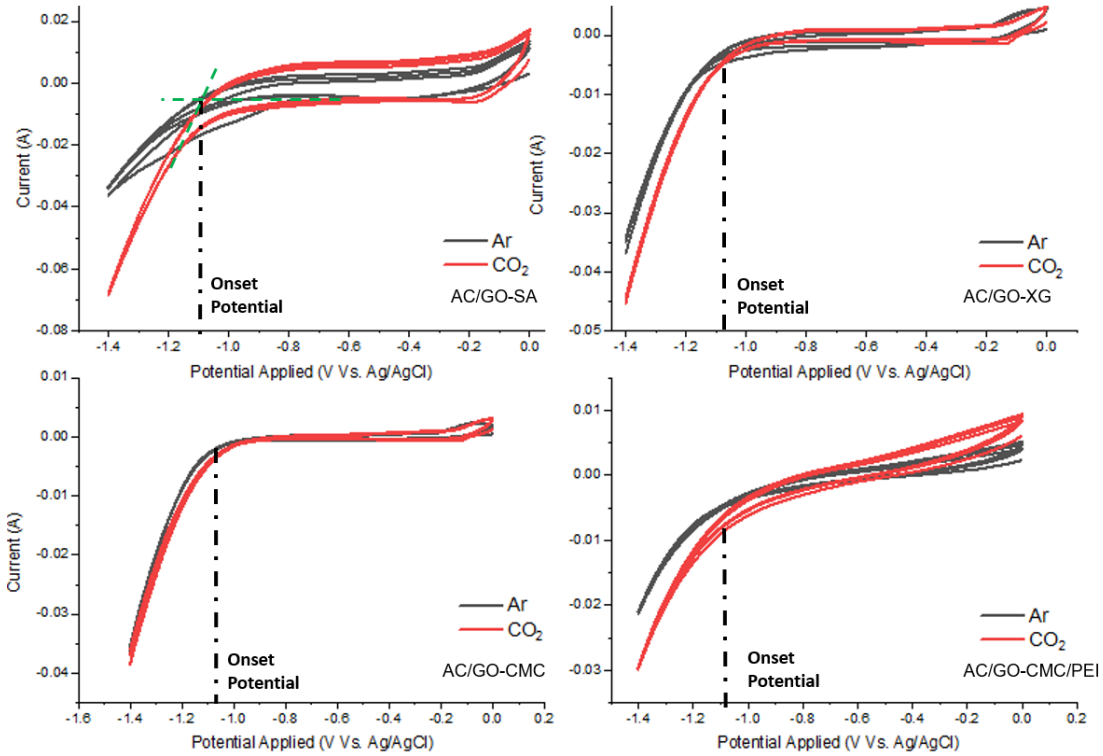

Figure 2: Cyclic voltammetry of AC/GO-x (where x = SA, XG, CMC and CMC/PEI) at the potential ranging between 0 to -1.4 V vs. Ag/AgCl

From Figure 2, the onset potential can be determined as well. This onset potential refers to the starting potential where all the thermodynamics and kinetic barriers are overcome, and an occurrence of the reduction (H_2 adsorption) process. The fast-rising current section of the peak is linearly extrapolated to the baseline and the intercept potential to obtain the onset potential as drawn in Figure 2 [23], [24]. The onset potential is selected to be applied for CA, since it is the lowest voltage for the reaction to begin, and to prevent a rapid reaction that will shift the reaction to the HER evolution. Referring to [25], the reduction of CO_2 to ethanol will go through multiple

steps of kinetic barriers and if the reaction is too hasty, the reaction will promotes H_2 evolution instead of CO_2RR. Upon the CV analysis, the research proceeds with CA analysis with applied potential of -1.1V *vs*. Ag/AgCl as all the electrodes showing an equivalent onset potential value. Figure 3 depicts the result of CA analysis for these electrodes at the selected onset potential. Herein, the CA analysis aims to study the stability of the reduction reaction such as kinetics of chemical reactions [26]. At t=0, the current is stepped up to reduce all the adsorbed species on the working electrode. Then, the current flow is controlled by rate of diffusion/adsorption process and the reaction that occur on the surface of working electrode [27].

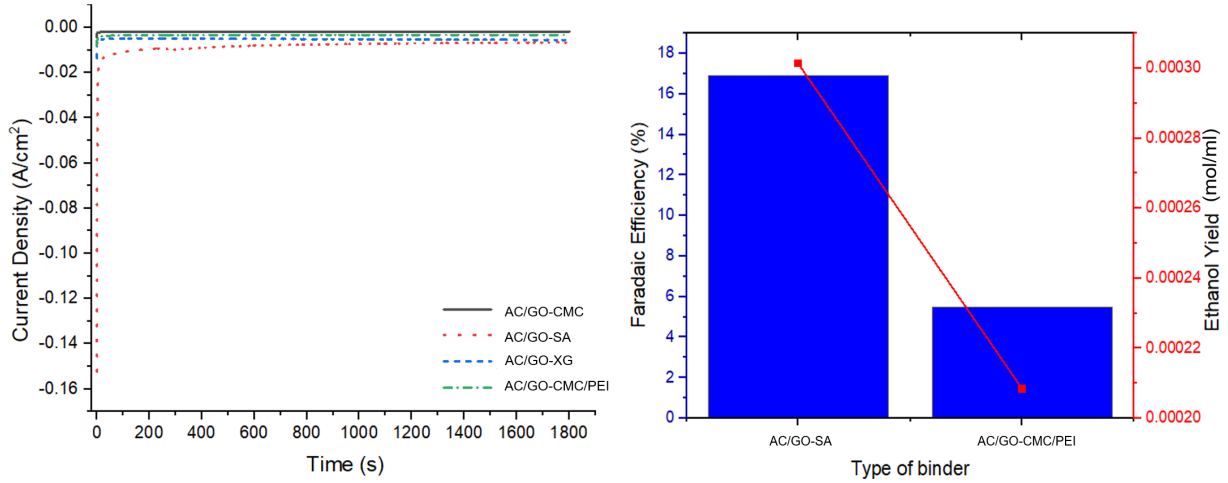

Figure 3: Chronoamperometry analysis (CA) at the potential of -1.1 V vs. Ag/AgCl for 30 mins (left). Faradaic efficiency and total ethanol yield for AC/GO-SA and AC/GO-CMC/PEI electrodes (right).

Based on Figure 3, AC/GO-SA shows the highest current density (cathodic) throughout the experiment, followed by AC/GO-XG, AC/GO-CMC/PEI and AC/GO-CMC with the corresponding value of 7.8, 5.1, 3.3 and 1.8 mA, respectively. The addition of PEI into CMC proves that mixed binder could increase the electrochemical performance as compared to the individual binders. Nevertheless, the produced current density is still lower when compared to AC/GO-SA, and AC/GO-XG. The poor performance of AC/GO-CMC/PEI is plausible due to high mixing ratio of the mixed polymeric binder as the amount of the binder affected the surface resistance of the electrodes [28]. If excess amount of binder is applied, it will slow down the ion transfer and if the opposite, the electrode cannot sustain its shape which both will led to higher current resistance.

Upon the completion of CA analysis, the liquid products are collected and sent for further analysis to determine the amount of ethanol formed. Figure 3 shows the Faradaic efficiency produced by AC/GO-SA and AC/GO-CMC/PEI, while ethanol is not detected by another two electrodes. However, due to poor understanding and lack of surface characterization, the precise explanation in term of the surface functionalities is still unknown. The formula of Faradaic efficiency is shown in Eq (2), where n is the amount of product detected, Q is the total charge passed during the electrolysis, F is the Faraday constant and Z is the number of electrons required to obtain 1 molecule of products which is 12 for ethanol [31]. According to literature study, [32] has managed to prepare zirconium oxide (ZrO_2) nanoparticles dispersed on N-doped carbon sheets by using SA and producing a promising FE value of 64% toward carbon monoxide (CO) production at low potential (-0.4 V *vs.* RHE). In 2022, [29] has successfully fabricated a single atom catalyst of nickel supported with carbon hydrogel by using CMC as binder. The working electrode work very well towards CO production at potential applied of -0.8V *vs.* RHE and resulting high FE (99.7%) with 226 mA/cm^2 current density. Besides, chitosan may also be used

as polymer binder to replace the synthetic binder. Research made by [30], shows that copper nanoparticle electrode combine with chitosan as polymer could produce high CO (FE = 93.7%) at potential -1.1V *vs.* RHE with 10 mA/cm^2 current density. Referring to Figure 3, the AC/GO-SA has exerted comparable current density (7.8 mA/cm^2) with the literature and sufficiently high Faradaic efficiency (16.9%) reported in literature for green binder towards ethanol production compared to AC/GO-CMC/PEI (5.4%)

$$\text{Faradaic efficiency (FE)} = \frac{n}{Q/ZF} = \frac{nZF}{Q} \quad (2)$$

Conclusion and way forward

In conclusion, the preliminary electrochemistry performance of an AC/GO composite electrode with green polymeric binder such as XG, SA, and CMC was tested in this work. According to physical analysis, CMC is the most adhesive polymeric binder among the others, with the lowest percentage mass loss (8.28%) during the investigation. This work also introduces a mixed polymer binder that is composed of PEI and CMC polymers. The combined polymer improves the coating material's adhesiveness. The electrochemical measurement of the fabricated electrode shows that AC/GO-SA caused a considerable anodic shift in CV while retaining a high current density (-7.8 mA/cm^2) during CA. Nevertheless, ethanol is only found for AC/GO-SA and AC/GO-CMC/PEI electrodes which has Faradaic efficiency of 16.9% and 5.4%, respectively. The preliminary studies show that CMC is a promising binder for coating due to the surface charges and intermolecular forces, while SA is able to produce better reaction toward the electrochemical reduction. Overall, the reaction towards electrochemical process is affected by the functional groups and crystal facet of the active material which will be explored further in future work.

Acknowledgement

The authors would like to acknowledge funding from the Ministry of Higher Education, Malaysia, under the HICoE grant (Grant no: 015MA0-052) and Universiti Teknologi PETRONAS for supporting the research.

References

[1] K. B. Karnauskas, S. L. Miller, and A. C. Schapiro, “Fossil Fuel Combustion Is Driving Indoor CO2 Toward Levels Harmful to Human Cognition,” *GeoHealth*, vol. 4, no. 5, 2020, https://doi.org/10.1029/2019GH000237

[2] K. O. Yoro and M. O. Daramola, CO2 emission sources, greenhouse gases, and the global warming effect. Elsevier Inc., 2020.

[3] J. Rissman *et al.*, “Technologies and policies to decarbonize global industry: Review and assessment of mitigation drivers through 2070,” *Appl. Energy*, vol. 266, no. March, p. 114848, 2020, https://doi.org/10.1016/j.apenergy.2020.114848

[4] S. Jin, Z. Hao, K. Zhang, Z. Yan, and J. Chen, “ Advances and Challenges for the Electrochemical Reduction of CO 2 to CO: From Fundamentals to Industrialization ,” *Angew. Chemie*, vol. 133, no. 38, pp. 20795–20816, 2021, https://doi.org/10.1002/ange.202101818

[5] J. H. Lee *et al.*, “Understanding the Role of Functional Groups in Polymeric Binder for Electrochemical Carbon Dioxide Reduction on Gold Nanoparticles,” *Adv. Funct. Mater.*, vol. 28, no. 45, pp. 1–6, 2018, https://doi.org/10.1002/adfm.201804762

[6] A. Pizzi, A. N. Papadopoulos, and F. Policardi, “Wood composites and their polymer binders,” *Polymers (Basel).*, vol. 12, no. 5, 2020, https://doi.org/10.3390/POLYM12051115

[7] C. Bauer, A. Bilican, S. Braxmeier, G. Reichenauer, and A. Krueger, "Sustainable supercapacitor electrodes based on preagglomerated carbon onions and a green binder," *Carbon N. Y.*, vol. 197, no. March, pp. 555–562, 2022, https://doi.org/10.1016/j.carbon.2022.06.041

[8] V. K. Thakur, M. K. Thakur, P. Raghavan, and M. R. Kessler, "Progress in green polymer composites from lignin for multifunctional applications: A review," *ACS Sustain. Chem. Eng.*, vol. 2, no. 5, pp. 1072–1092, 2014, https://doi.org/10.1021/sc500087z

[9] A. Khan, A. Rashid, R. Younas, and R. Chong, "A chemical reduction approach to the synthesis of copper nanoparticles," *Int. Nano Lett.*, vol. 6, no. 1, pp. 21–26, 2016, https://doi.org/10.1007/s40089-015-0163-6

[10] M. Farhan, H. Othman, H. Hafiy, M. Azmi, and N. Adilla, "Materials Today : Proceedings '' One-pot " synthesis of activated carbon – Graphene oxide polyethyleneimine-functionalized supported copper nanoparticles electrode for carbon dioxide reduction reaction," *Mater. Today Proc.*, no. xxxx, 2022, https://doi.org/10.1016/j.matpr.2022.03.048

[11] Z. Ge and Z. He, "An effective dipping method for coating activated carbon catalyst on the cathode electrodes of microbial fuel cells," *RSC Adv.*, vol. 5, no. 46, pp. 36933–36937, 2015, https://doi.org/10.1039/c5ra05543a

[12] H. N. Yang, J. S. Park, S. Y. Jeon, and K. H. Park, "Carboxymethylcellulose (CMC) formed nanogels with branched poly(ethyleneimine) (bPEI) for inhibition of cytotoxicity in human MSCs as a gene delivery vehicles," *Carbohydr. Polym.*, vol. 122, pp. 265–275, 2015, https://doi.org/10.1016/j.carbpol.2014.12.073

[13] G. Folaranmi, M. Bechelany, P. Sistat, M. Cretin, and F. Zaviska, "Comparative investigation of activated carbon electrode and a novel activated carbon/graphene oxide composite electrode for an enhanced capacitive deionization," *Materials (Basel).*, vol. 13, no. 22, pp. 1–14, 2020, https://doi.org/10.3390/ma13225185

[14] S. Dhibar and C. K. Das, "Silver nanoparticles decorated polypyrrole/graphene nanocomposite: A potential candidate for next-generation supercapacitor electrode material," *J. Appl. Polym. Sci.*, vol. 134, no. 16, pp. 1–14, 2017, https://doi.org/10.1002/app.44724

[15] Z. Y. Sui, Y. Cui, J. H. Zhu, and B. H. Han, "Preparation of Three-dimensional graphene oxide-polyethylenimine porous materials as dye and gas adsorbents," *ACS Appl. Mater. Interfaces*, vol. 5, no. 18, pp. 9172–9179, 2013, https://doi.org/10.1021/am402661t

[16] W. Li *et al.*, "Preparation and Characterization of Beads of Sodium Alginate/Carboxymethyl Chitosan/Cellulose Nanofiber Containing Porous Starch Embedded with Gallic Acid: An In Vitro Simulation Delivery Study," *Foods*, vol. 11, no. 10, 2022, https://doi.org/10.3390/foods11101394

[17] J. M. A. Alsharef, M. R. Taha, and T. A. Khan, "Physical dispersion of nanocarbons in composites – A review," *J. Teknol.*, vol. 79, no. 5, pp. 69–81, 2017, https://doi.org/10.11113/jt.v79.7646

[18] J. Zhang *et al.*, "An overview of the characteristics of advanced binders for high-performance Li–S batteries," *Nano Mater. Sci.*, vol. 3, no. 2, pp. 124–139, 2021, https://doi.org/10.1016/j.nanoms.2020.10.006

[19] S. Zhang *et al.*, "Polyethylenimine-enhanced electrocatalytic reduction of CO2 to formate at nitrogen-doped carbon nanomaterials," *J. Am. Chem. Soc.*, vol. 136, no. 22, pp. 7845–7848, 2014, https://doi.org/10.1021/ja5031529

[20] X. Li *et al.*, "Efficient CO2 capture by functionalized graphene oxide nanosheets as fillers to fabricate multi-permselective mixed matrix membranes," *ACS Appl. Mater. Interfaces*, vol. 7, no. 9, pp. 5528–5537, 2015, https://doi.org/10.1021/acsami.5b00106

[21] S. Das *et al.*, "Core-shell structured catalysts for thermocatalytic, photocatalytic, and electrocatalytic conversion of CO2," *Chem. Soc. Rev.*, vol. 49, no. 10, pp. 2937–3004, 2020, https://doi.org/10.1039/c9cs00713j

[22] Z. Kou *et al.*, "Fundamentals, On-Going Advances and Challenges of Electrochemical Carbon Dioxide Reduction," *Electrochem. Energy Rev.*, vol. 5, no. 1, pp. 82–111, 2022, https://doi.org/10.1007/s41918-021-00096-5

[23] A. J. R. Botz, M. Nebel, R. A. Rincón, E. Ventosa, and W. Schuhmann, "Onset potential determination at gas-evolving catalysts by means of constant-distance mode positioning of nanoelectrodes," *Electrochim. Acta*, vol. 179, pp. 38–44, 2015, https://doi.org/10.1016/j.electacta.2015.04.145

[24] R. Sanchis-Gual, A. Seijas-Da Silva, M. Coronado-Puchau, T. F. Otero, G. Abellán, and E. Coronado, "Improving the onset potential and Tafel slope determination of earth-abundant water oxidation electrocatalysts," *Electrochim. Acta*, vol. 388, p. 138613, 2021, https://doi.org/10.1016/j.electacta.2021.138613

[25] L. Li, Y. Huang, and Y. Li, "Carbonaceous materials for electrochemical CO2 reduction," *EnergyChem*, vol. 2, no. 1, p. 100024, 2020, https://doi.org/10.1016/j.enchem.2019.100024

[26] R. K. Franklin, S. M. Martin, T. D. Strong, and R. B. Brown, *Chemical and Biological Systems: Chemical Sensing Systems for Liquids*, no. May 2015. Elsevier Ltd., 2016.

[27] F. Scholz, Electroanalytical methods: Guide to experiments and applications. 2010.

[28] Y. K. Lee, "The effect of active material, conductive additives, and binder in a cathode composite electrode on battery performance," *Energies*, vol. 12, no. 4, 2019, https://doi.org/10.3390/en12040658

[29] H. Guo, D.-H. Si, H.-J. Zhu, Q.-X. Li, Y.-B. Huang, and R. Cao, "Ni single-atom sites supported on carbon aerogel for highly efficient electroreduction of carbon dioxide with industrial current densities," *eScience*, vol. 2, no. 3, pp. 295–303, 2022, https://doi.org/10.1016/j.esci.2022.03.007

[30] A. Marcos-Madrazo, C. Casado-Coterillo, J. Iniesta, and A. Irabien, "Use of Chitosan as Copper Binder in the Continuous Electrochemical Reduction of CO2 to Ethylene in Alkaline Medium," *Membranes (Basel).*, vol. 12, no. 8, p. 783, 2022, https://doi.org/10.3390/membranes12080783

[31] E. O. Eren and S. Özkar, "Recent advances in heterogeneous catalysts for the effective electroreduction of carbon dioxide to carbon monoxide," *J. Power Sources*, vol. 506, no. June, 2021, https://doi.org/10.1016/j.jpowsour.2021.230215

[32] Z. Miao, P. Hu, C. Nie, H. Xie, W. Fu, and Q. Li, "ZrO2 nanoparticles anchored on nitrogen-doped carbon nanosheets as efficient catalyst for electrochemical CO2 reduction," *J. Energy Chem.*, vol. 38, pp. 114–118, 2019, https://doi.org/10.1016/j.jechem.2019.01.010